Volume 1 | Number 1 | Jan 2013 | Pages 1–100

Analyst

www.rsc.org/analyst

ROYAL SOCIETY OF CHEMISTRY

ROYAL SOCIETY OF CHEMISTRY

www.rsc.org/analyst

The use of Ion Mobility Mass Spectrometry to assist Protein Design: a Case Study on Zinc Finger Fold *versus* Coiled Coil Interactions

Yana Berezovskaya[b], Massimiliano Porrini[b,1], Chris Nortcliffe[a], and Perdita E Barran*[a]

[a] The School of Chemistry, Manchester Institute of Biotechnology,
The University of Manchester, Manchester, UK
[b] School of Chemistry, University of Edinburgh, Edinburgh, UK

* Corresponding author (Perdita.Barran@manchester.ac.uk)

Abstract

The dramatic conformational change in zinc fingers on binding metal ions for DNA recognition makes their structure-function behaviour an attractive target to mimic in *de novo* designed peptides. Mass spectrometry, with its high throughput and low sample consumption provides insight into how primary amino acid sequence can encode stable tertiary fold. We present here the use of ion mobility mass spectrometry (IM-MS) coupled with molecular dynamics (MD) simulations as a rapid analytical platform to inform *de novo* design efforts for peptide-metal and peptide-peptide interactions. A dual peptide-based synthetic system, ZiCop based on a zinc finger peptide motif, and a coiled coil partner peptide Pp, have been investigated. Titration mass spectrometry determines the relative binding affinities of different divalent metal ions[1] as $Zn^{2+} > Co^{2+} \gg Ca^{2+}$. With collision induced dissociation (CID), we probe complex stability, and establish that peptide-metal interactions are stronger and more 'specific' than those of peptide-peptide complexes, and the anticipated hetero-dimeric complex is more stable than the two homo-dimers. Collision cross-sections (CCS) measurements by IM-MS reveal increased stability with respect to unfolding of the metal-bound peptide over its apo-form, and further, larger collision cross sections for the hetero-dimeric forms suggest that

1

dimeric species formed in the absence of metal are coiled coil like. MD supports these

structural assignments, backed up by data from visible light absorbance measurements.

Introduction

One of the important goals of protein design is to replicate, from first principles, active folds, and on doing this synthesise small functional candidates, that may perform useful tasks[2]. The usual approach involves careful consideration of which active fold(s) are required, identification of the minimal sequence features to retain fold, followed by iterative design[3]. Assessing whether a given design strategy has been successful in obtaining the correct fold, will usually be achieved with several analytical biophysical characterisation methods, with mass spectrometry usually only employed to obtain the weight (and perhaps purity) of the synthesised component(s). However developments in soft ionisation techniques[4], and in particular in electrospray ionisation[5] have enabled researchers to analyse intact protein complexes in the gas phase, determine stoichiometries and detail interactions of systems of increasing complexity[6]. Collision induced dissociation can be applied to interrogate the strength of interaction between protein complex subunits[7, 8]. It has also become possible to determine conformations of proteins and their complexes using a related technique termed ion mobility mass spectrometry (IM-MS)[9-11]. These mass spectrometry based approaches to determining structure represent an attractive rapid route to analysis that might form part of a protein design platform.

In this work we present an analytical workflow that can be used to characterise and test *de novo* designed peptides. As an example system we take a peptide that attempts to encode two different sequences for two distinct folds simultaneously; the transition between the conformational states is reversible and is triggered by specific metal binding. Our characterisation platform has been developed to interrogate stoichiometry of binding, metal affinity, fold, conformational transitions, and the strength of interactions between hetero-dimers. We use mass spectrometry (MS) ion mobility mass spectrometry (IM-MS), molecular dynamics and solution based measurements. This workflow is illustrated in Figure 1 along with examples which appear later in this paper.
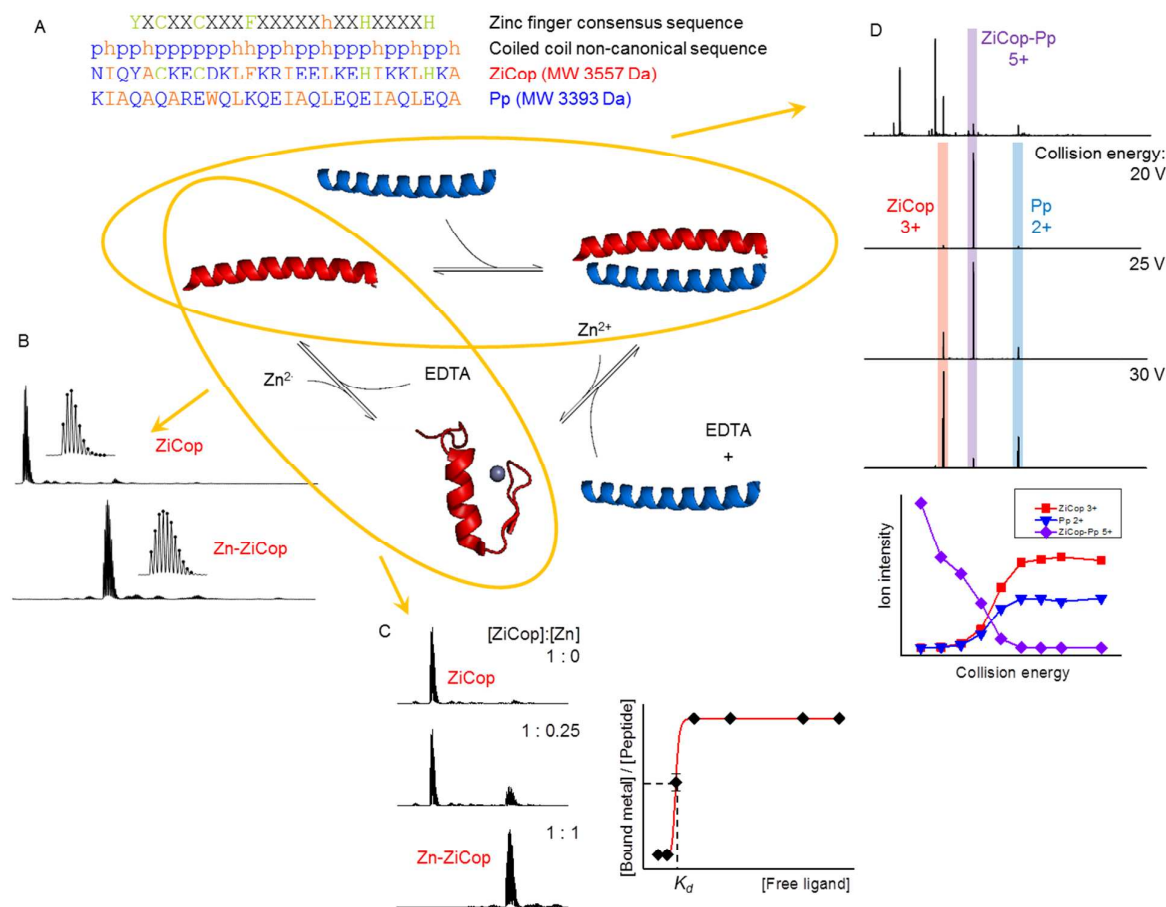
3

Figure 1. Design concept of the dual reversible peptide-based switch. A – Sequence of the ZiCop and its binding partner Pp in relation to the structural requirements for the zinc finger and coiled coil designs. The 'X' refers to any amino acid, 'h' – to any hydrophobic residue, 'p' – to any polar residue. Below is proposed switching process: the red peptide represents ZiCop, which is responsive to zinc; the partner peptide (blue) was designed to interact with ZiCop in the absence of zinc. B through D – A schematic representing analytical workflow of the design concept interrogation using MS platform. B – Stoichiometry of binding (top spectrum: free ZiCop peak, bottom: Zn-bound peptide). C – Quantification of affinity of the peptide to the metal ion (mass spectra of Zn titrations into ZiCop and resulting biding curve to yield dissociation constant). D – Evaluation of the hetero-dimeric coiled coil association using collisionally induced dissociation (CID); resulting curves indicate survival of the precursor ion of the coiled coil (purple) and formation of the products – ZiCop and Pp (red and blue respectively).

The two conformations of the test switching system are a zinc finger fold and a coiled-coil motif. The choice has been dictated by the fact that the rules governing the folds are extensively studied, so the novel bio-orthogonal systems can be designed confidently. Also, both folds are independent, stable and well-defined motifs. The reversible switch between the two conformational states is controlled by the binding of a metal ion, zinc, to the peptide. The

4

aim of synthesis was that the peptide, named ZiCop (reflecting the structural duality of <u>zi</u>nc finger and <u>co</u>iled-coil <u>p</u>eptide), in the absence of the Zn^{2+} ions would form and amphipathic parallel dimeric helix for coiled-coil interactions with a <u>p</u>artner <u>p</u>eptide (Pp), then with the addition of Zn^{2+} form a metal-bound monomer adopting a zinc finger conformation. The system can be switched back to the coiled-coil interactions through the removal of Zn^{2+} using EDTA.[1]

The zinc finger proteins were amongst the earliest reported gene-specific eukaryotic transcription factors [12]. They possess a repeating motif which is involved with binding of DNA, and also associated with zinc binding, which led to the name 'zinc finger'. Misfolding of zinc finger proteins has been linked to a variety of human diseases such as cancer and a series of neural disorders [13], highlighting a need to study the structural stability of this motif. There are several different classes of zinc finger fold [14] each with a different structural motif although all involve cysteine and histidine residues binding the zinc ion. A hydrophobic cluster is also conserved within most zinc fingers. The zinc ion is a vital component in stabilising the structure of these proteins: in its absence the protein has a different structural conformation. The first discovered and most common zinc finger motif is Cys_2His_2. The domains adopt a $\beta\beta\alpha$ fold and binds with the major groove of DNA at 3 base pair intervals[15] through several amino acid residues. A series of hydrophobic residues are also conserved within most members of this group with Tyr6 (or Phe6), Phe17, and Leu23 being retained[16]. The most common task associated with this class of zinc finger is regulation of transcription[17].

The other peptide system we assess here is the coiled-coil motif. This system was first suggested by Crick in 1953[18] to describe packing in α-keratin but has been applied to the packing between any 2 to 7 α-helices. The molecular structure of the coiled-coil motif is a set of repeating residues of the form *hpphppp*, of hydrophobic (*h*) and polar (*p*). This heptad repeating pattern spaces the hydrophobic amino acids every three to four residues apart allowing one turn between them at 3.6 amino acids per turn producing an amphipatic helix. The hydrophobic faces of the α-helices interact to form a supra-molecular coil structure leaving

the polar residues exposed for interaction with other molecules. Coiled-coil interactions are inherently non-specific rather than being due to some active site, this leads the constituent α-helices to orientate in a variety of ways in misaligned bundles and aggregates[19]. The coiled-coil motif is an interesting system for protein design efforts, providing information on protein folding and interactions as well as in *de novo* design. To specify a coiled-coil sequence, hydrophobic residues need to be spaced 3 to 4 residues apart (Figure 1A). Specifying the oligomeric state of the coiled-coil, however, is a more complicated task [20], and is not based on the sequence alone, but on the global energy minimum of a specific protein with a coiled-coil domain. Despite this latter complication, the basic design rules for parallel dimeric coiled-coils have been well established based on the vast body of information collected on these sequences [21, 22].

Mass spectrometry can provide useful insights into protein conformational changes. The gentle process of nano-electrospray ionisation (nESI) preserves non-covalent interactions enabling studies of protein-ligand and protein-protein interactions. The number of available ionisable sites on the protein is used as a measure of 'unfoldedness' of the conformation [23]. High sensitivity (down to femtomolar concentrations), dynamic range ($\sim 10^6$) and selectivity of MS also allows monitoring of many/all components at once [24] [25] [26]. Many biochemical processes reach equilibration within a few seconds after initiation, which renders monitoring of such processes before the equilibrium is established inaccessible by other techniques. The millisecond time-scales of MS-based techniques offer an attractive alternative to study non-equilibrium states of protein systems and fast dynamical processes [27]. MS-based approaches offer a range of additional tools to interrogate the system under investigation. For example, collision induced dissociation can be applied to interrogate the arrangement of sub-units in the protein complex and the strength of interaction between them[28].

IM-MS allows users to calculate collision cross sections and hence obtain valuable information on conformations adopted in the gas phase[9]. Ion mobility adds an extra dimension to mass spectrometry, as it can resolve structural isomers[29], probe non-covalent interactions[30]

and monitor catalytic activity[31]. Ion mobility data can be interpreted with the help of molecular modelling, whereby theoretical collision cross section of a protein can be compared to experimental values. Based on this comparison, candidate geometries can be proposed. Mass spectrometry and ion mobility mass spectrometry can be used to study sequence-to-structure relationships, in the absence of solvent; conformations of small peptides preserved *in vacuo* are defined mainly by the sequence [32, 33].

In ion mobility mass spectrometry (IM-MS), a pulse of molecular ions formed by nESI process is injected into a drift cell which possesses a weak electrostatic field and is filled with an inert buffer gas. Ions drift due to the field, and are retarded due to collisions with the buffer gas. The time it takes ions to traverse this drift cell is related to their charge and shape, and each ion will have a measurable mobility (K) the constant of proportionality between the drift velocity (v_d) and the electric field (E). By measuring the arrival time distribution of ions at a detector – usually following mass analysis – it is possible to determine the K and from that derive the buffer gas and temperature dependent rotationally averaged collision cross section of ions (CCS) (Ω) according to Equation 1 below.

$$K = \frac{3ze}{16N}\sqrt{\frac{2\pi}{\mu k_B T}}\frac{1}{\Omega}$$

Equation 1

Where K is the measured mobility on an ion, z is the ion charge state, e is the elementary charge, N is the gas number density, μ is the reduced mass of the ion-neutral pair, k_B is the Boltzmann constant and T is the gas temperature.

Determining the CCS allows us to elucidate conformations adopted in the gas phase[29, 34] which can be related to solution conformations. Experimentally derived CCS, and hence conformations, can be complemented by MD analysis to atomistically resolve the structures [35-37]. IM-MS has been successfully applied in fundamental studies of sequence-to-structure relationships in polypeptides, since structures observed *in vacuo* are defined intrinsically by the sequence[1, 32, 33]. In this study we use IM-MS coupled with MD to determine the conformations

of peptides and their complexes, we explore the use of this technique as a tool to assist protein

design to encode fold from primary sequence.

Experimental Section

Materials

Both peptides reported here – ZiCop and Pp, were synthesised on a microwave-assisted peptide synthesiser (Liberty CEM) employing standard solid-phase Fmoc-based peptide synthesis techniques. The corresponding sequences are shown in Figure 1.

Peptides were purified using reverse phase high performance liquid chromatography (HPLC) performed using a JASCO PU980 HPLC system in conjunction with reverse-phase C18 or C4 columns. Identities of peptides were confirmed by matrix assisted laser desorption ionisation time of flight (MALDI-ToF) mass spectrometry, performed on a 4700 TOF/TOF™ instrument (Applied Biosystems). Protein concentrations were measured on a PerkinElmer Lambda-25 spectrophotometer, and determined using Beer's law. The binding of zinc was shown to be reversible in solution phase spectroscopic assays *via* the use of EDTA.[38]

LC-MS grade solvents and ammonium acetate were purchased from Fisher (Loughborough, UK). Metal salts (cobalt and calcium acetates) and the control peptides substance P, melittin and bradykinin were obtained from Sigma Aldrich (Dorset, UK) and zinc acetate was obtained from Fisons (Loughborough, UK), and used without further purification. Prior to all MS and IM-MS studies all cysteine-containing peptides were incubated for ~1 min with a 10-fold molar excess of TCEP to selectively reduce any potential disulphide bond formation. Peptides were used in 50 μM concentrations and sprayed into the mass spectrometer from the 'buffered' conditions, *i.e.* in 20 mM ammonium acetate and 5% isopropyl alcohol. The solution pH was adjusted to 7.2. These solution conditions had been optimised in our earlier work[1] on a similar peptide system.

NanoESI-MS analysis

Mass spectra were obtained using a Waters Micromass hybrid quadrupole time of flight mass spectrometer Q-ToF-2 (Manchester, UK) equipped with an orthogonal nano-electrospray source. Source parameters were optimised to retain non-covalent interactions and maintained for all experiments. Typical source operating values were: capillary voltage ~1 kV, source temperature 80 °C. All experiments were performed in triplicate and mean values are reported.

Calculation of dissociation constants

Calculation of K_d using gas-phase titrations of the peptide with one ligand, along with two-ligand competitive binding experiments, uses the approach described by Sannes-Lowery and co-workers[39]. Using nESI-MS, the stoichiometry and relative abundance of the apo-peptide and the peptide-metal complex can be determined simultaneously *via* their first monoisotopic peak intensities. More details on the methodology can be found in supplementary information.

Collision cross sections measurements

IM-MS experiments were carried out on the MoQ-ToF (<u>mo</u>bility <u>q</u>uadrupole <u>t</u>ime <u>of</u> <u>fl</u>ight) instrument, which is a Waters Micromass Q-ToF quadrupole time-of-flight mass spectrometer modified from the original by inclusion of a drift cell[40]. During ion-mobility separation, desolvated ions are injected into the drift cell. The electric potential is sequentially ramped down from 60 to 20 V with a step of 10 V for the first three settings and with a step of 5 V from then on. For each voltage setting, a total of 10 ion-mobility separations are summed and mass spectra of all arrival-time distributions were recorded synchronously with the injection of ions into the cell. Experimental arrival times were plotted against *P/T*, and rotationally average collision cross-sections of all analyte ions obtained using the theory described earlier[9, 40, 41]. Each experiment was carried out in triplicate and the final result is reported as the mean collision cross section.

Molecular dynamics simulations

Force field measurements were carried out using the Amber 10 modelling package implementing Amber99 force field. The ionisation state of the peptides was assigned as it would be in solution at pH 7 using the H++ algorithm [42]. The time step for the simulations *in vacuo* was 0.5 fs (as no constraints were applied). Following minimisation and thermalisation at 300 K of the structures, production runs were carried out in a canonical ensemble for up to 10 ns. The nonbonded [43] model was adopted to simulate the interaction of the Zn ligand with ZiCop, which uses only electrostatic and van der Waals forces. The resulting structures of ZiCop and Zn-ZiCop were subjected to simulated annealing to probe a wider conformational space for the candidate geometries. The lowest energy structure found within the band of experimental cross section values was selected to calculate MD collision cross sections with the MobCal program [35, 36] employing the trajectory method.

Results and Discussion

1. Overview of the interactions – stoichiometry of binding

Under the experimental conditions described above, the ZiCop peptide presents three ions of the general form $[ZiCop+nH]^{n+}$ with n = 3-5, (Figure 2*A*), with $[ZiCop+4H]^{4+}$ being the most dominant. The Partner peptide Pp also presents these charge states, but here $[Pp+3H]^{+3}$ is more dominant (Figure 2*B*). In both cases, a homo-dimer is observed predominantly as a $[2M+5H]^{5+}$ ion. Isotopic cluster analysis suggests that a smaller amount of the $[2M+4H]^{4+}$ ion is also present, but this is *m/z*-coincident with low abundant $[M+2H]^{2+}$ monomer.

When the two peptides are mixed together in equimolar amounts (Figure 2*C*), a small peak at *m/z* 1391.0 is observed corresponding to the hetero-dimer $[Pp:ZiCop+5H]^{5+}$. The relatively low intensity of this species, compared with that of the homo-dimers suggests that the interactions between the two peptides are not particularly strong. Addition of zinc to the peptides, to give equimolar amounts of each component (Figure 2*D*), yields full binding of the ZiCop peptide to the metal, accompanied by the loss of the $[ZiCop+5H]^{5+}$ species, suggesting a

10

more compact conformation with less protonatable groups accessible to solvent. In addition, in

the presence of zinc, the (now metal bound) monomeric ZiCop species drops in intensity

relative to the Pp. Interestingly, the zinc-bound form of the ZiCop tends to form a dimer and

also to interact with Pp, with the latter effect supported by spectroscopic measurements in

solution. [38] In order to confirm that the binding of ZiCop to the partner peptide is specific we

performed a series of control experiments where we incubated ZiCop with three other peptides,

bradykinin 1-7, melittin and substance P, under the same conditions as for the partner peptide

(supplementary information Figure S1). For these experiments no complex was observed.
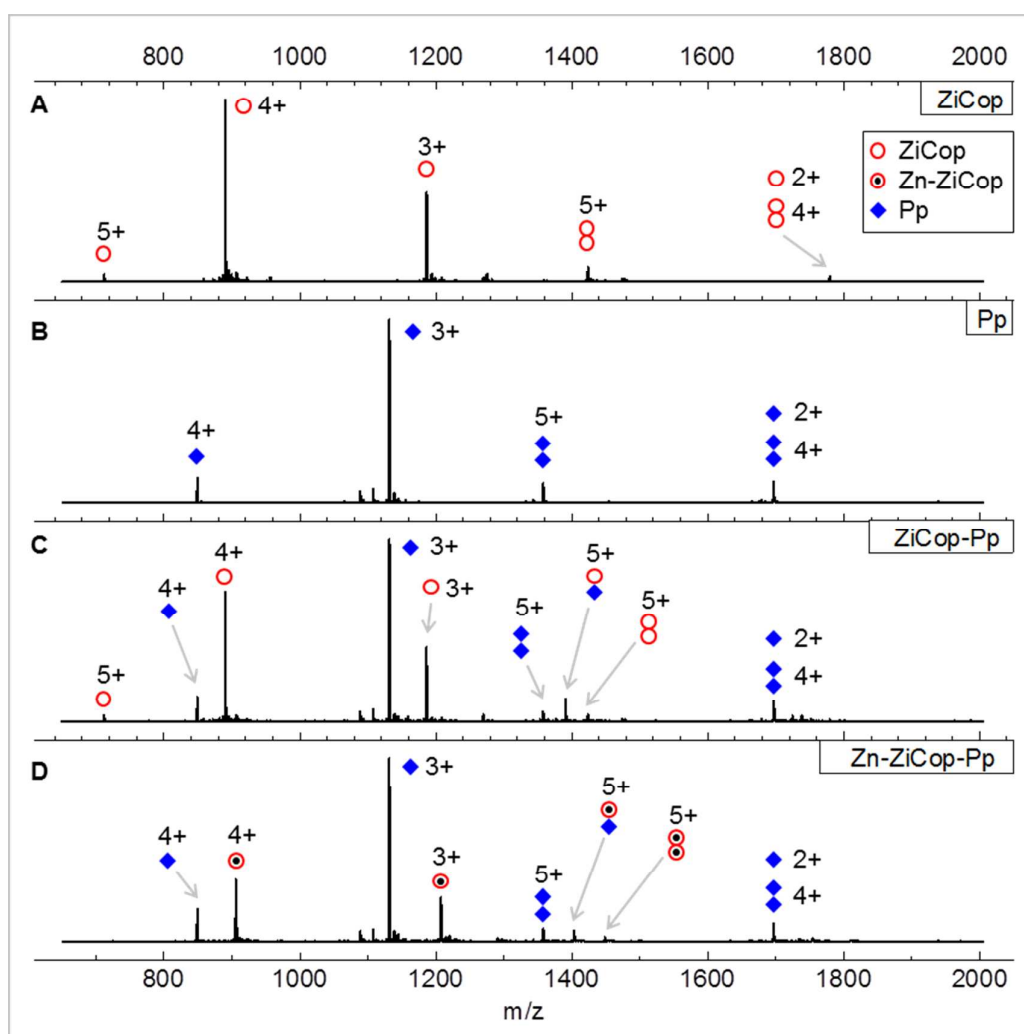

Figure 2   *Representative nESI mass spectra of ZiCop and the partner peptide (Pp) obtained individually and mixed in the absence and presence of zinc. A and B – ZiCop and Pp respectively sprayed from the buffered conditions (see below); C – equimolar mixture of ZiCop and Pp, featuring monomeric and dimeric species; D – equimolar mixture of ZiCop, Pp and zinc acetate featuring full zinc binding by ZiCop and aggregation events .*

11

Conditions: 50 µM peptides and zinc acetate, 20 mM ammonium acetate, 5% isopropanol, 500 µM TCEP, pH 7.2. The peaks are denoted as follows (see legend in pane A: one for all spectra): apo-ZiCop by red circles, Zn-bound ZiCop by red circles with a black dot in the centre, Pp by blue diamonds, and any dimeric species are shown by clusters of relevant shapes.

2. *Metal ions and ZiCop - quantifying metal-ion affinity*

Figure 3 shows a typical nESI mass spectra obtained for ZiCop without (Figure 3*A*) and with (Figure 3*B-D*) equimolar amounts of metal salts added (with the exception of calcium acetate whose concentration was quadruple that of the peptide); the regions for the +4 charge states of the peptide are shown with an insert zoomed to show isotopic resolution. $[ZiCop+4H]^{4+}$ or the equally charged $[ZiCop+X+2H]^{4+}$, where X = divalent cation, are the dominant peaks in the spectra, twice as intense as $[ZiCop+3H]^{3+}$. Use of TCEP (tris(2-carboxyethyl)-phosphine) maintained approximately 99% of the cysteines in their reduced state as evidenced by isotopic cluster analysis. Theoretical fits to the elemental compositions of the fully reduced peptide are superimposed on the experimental isotopic distribution (inserted spectra Figure 3), which allowed us to conclude that under these conditions the metals are coordinated by thiolates ($–S^-$).

The ratio between the intensity of the ^{12}C peak for both apo and holo species was determined for each spectrum, which shows that ZiCop has highest affinity for cobalt, a comparative high affinity for zinc and a significantly lower affinity for calcium: $Co^{2+} > Zn^{2+} \gg Ca^{2+}$. This is similar to the data found for a model zinc finger in our earlier work [1], although for that system the zinc affinity was marginally higher than that for cobalt. Just under 20% of the ZiCop is bound in the presence of Zn^{2+} (Figure 3*B*) and a quarter of the peptide population remains unbound in the presence of Co^{2+} (Figure3*C*). A very low fraction of ZiCop (less than 10%) is associated with Ca^{2+} (Figure3*D*). Addition of either Zn^{2+} or Co^{2+} narrows the charge state distribution of ZiCop in favour of the 4+ charge state (spectra not shown), which suggests metal-induced stabilisation of the fold.
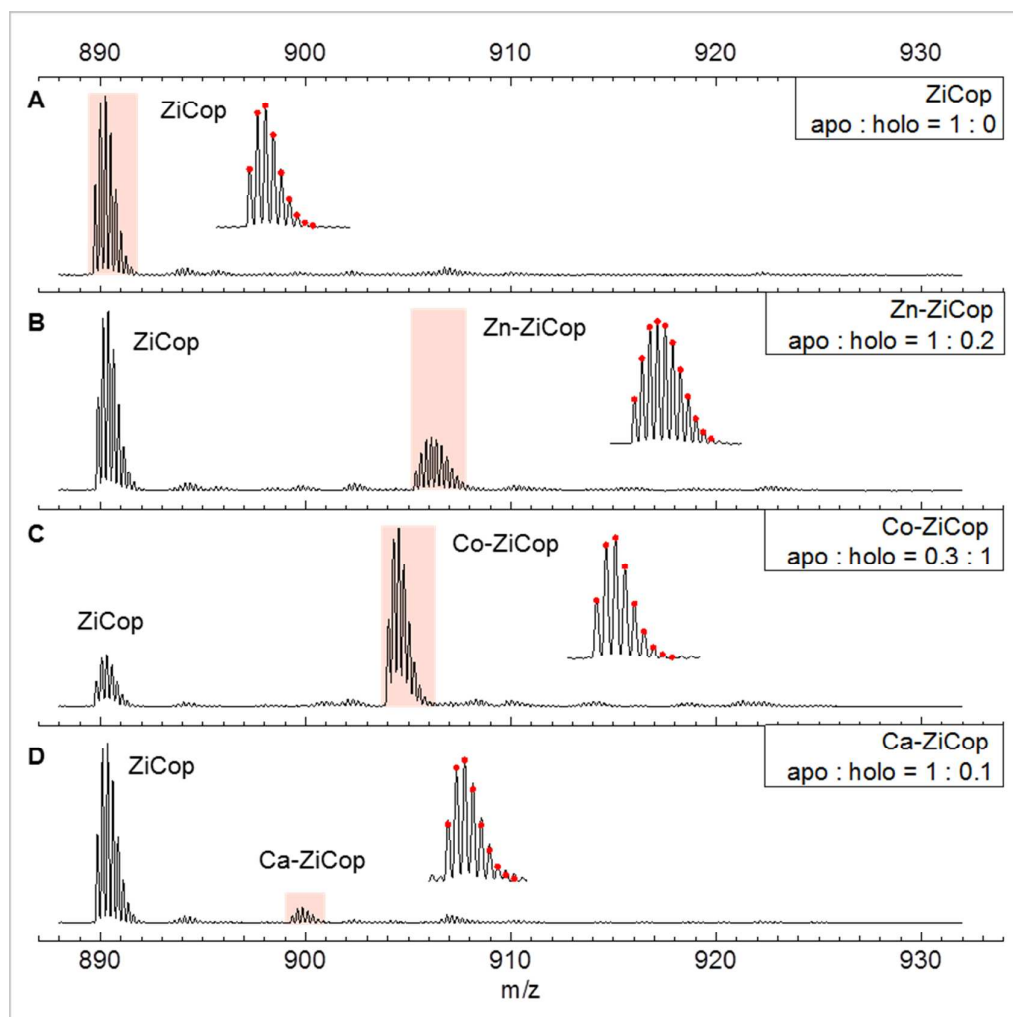
Figure 3 *Representative nESI mass spectra of the +4 charge state of ZiCop for: (A) the apo state, and with: (B) Zn^{2+}, (C) Co^{2+} and (D) Ca^{2+}. Ratios of apo to holo form are calculated from the intensities of the mono-isotopic peaks (first monoisotopic peak in each series). Insets show the resolved isotopic clusters for the free and bound states (highlighted regions on the mass spectra) along with theoretical fitting (denoted by dots ●). Isotopic cluster analysis indicated that 99% of the peptide is reduced. Conditions: 50 μM peptide; 20 mM ammonium acetate; 5% isopropanol; pH 7.2; 500 μM TCEP; 50 μM metal acetate salts for Zn and Co, and 200 μM for Ca.*

In order to determine the K_d for metal binding, all charge states were considered. The following assumptions are made when calculating K_ds from ESI –MS measurements [39, 44, 45]:

(i)   The mass and size of the ligand (metal ion in the case here) is small relative to the target peptide, so its contribution (negative or positive) to the overall ionisation efficiency is negligible when comparing free and bound peptide.

(ii)   Peak intensities from mass spectra correlate to concentrations in solution at the relatively low concentrations that are used for nESI-MS, as this method preserves

13

non-covalent interactions in complexes, when used correctly. Consequently, the relative ratios of bound *versus* non-bound target are considered to reflect the ratios in solution. This latter point depends on the interaction strength, but is likely to hold for electrostatic interactions as we have here.

In this study, the intensity of the first monoisotopic peak is chosen as a measure of concentration, due to its ease of implementation. Preliminary experiments (data not shown) demonstrated that this method yields comparable results to the more laborious integration of the area under the peak. The second metal ion binding to the ZiCop were neglected as the intensities were less than 5% of the first metal binding species except in the case of calcium, where at times it was up to 10 %.

Figure4 A-C shows binding curves obtained for ZiCop complexed by Zn, Co, and Ca respectively. In good agreement with the results presented above, strong binding is observed for Zn^{2+} and Co^{2+} (with K_ds of 41 ± 2 and 17 ± 3 μM, respectively), and very poor for Ca^{2+} (K_d = 714 ± 45 μM). The sigmoidal shape of the zinc- and cobalt-binding curves, as well as the value of $n > 1$, suggests switching behaviour of ZiCop when presented with Zn^{2+} or Co^{2+} cation. Figure 4D shows the binding curve obtained by titrating Zn^{2+} into ZiCop equilibrated with an equimolar concentration of Co^{2+}. The curve has a negligible lag phase, suggesting tight binding. Competitive titrations between Zn^{2+} and Co^{2+} revealed a stronger zinc affinity to ZiCop (K_d = 2 ± 0.3 μM) compared to cobalt, than for Zn^{2+} titrated individually. This suggests not only that Zn^{2+} easily displaces Co^{2+}, but also that the presence of the latter 'configures' the binding site of the ZiCop for coordinating Zn^{2+}. Although the curve has a quasi-hyperbolic shape, the value of n > 1 indicates switching behaviour at the concentrations below the detection limit of the method employed. The competition experiment performed the 'opposite' way, *i.e.* by titrating cobalt into zinc-bound ZiCop (1:1 stoichiometry) reveals Zn^{2+} is not displaced by Co^{2+} even at 5-fold molar excess of cobalt acetate. This is strong evidence that ZiCop preferentially and specifically binds Zn^{2+} in the presence of Co^{2+}. Previously reported ESI-MS studies demonstrated that the order of affinity of different metals for calmodulin was

14

altered in the presence of calcium, [46], in that work the binding affinity of the protein for lead

was enhanced in the presence of calcium, here a similar effect is shown for zinc in the presence
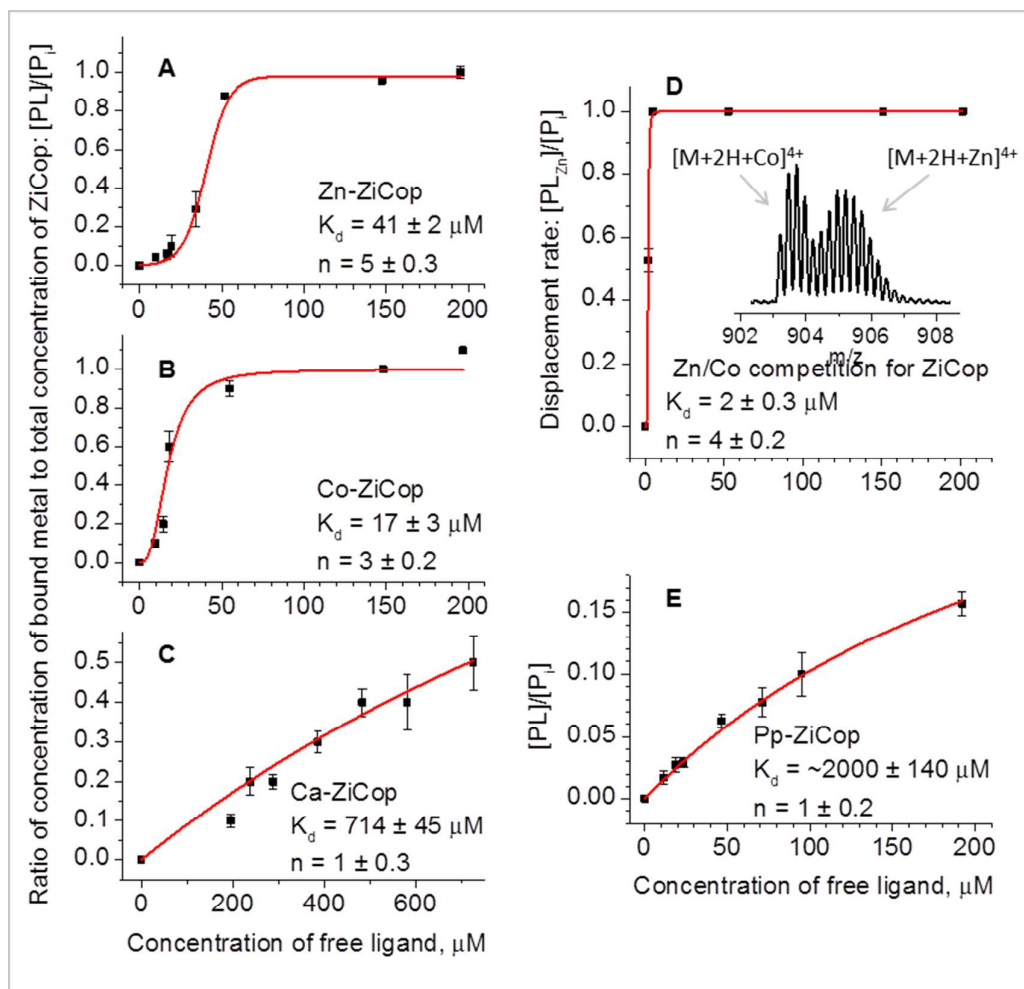
of cobalt.

Figure 4   *Titration curves of ZiCop against metals and Partner Peptide obtained from titration nESI-MS*
experiments: (A) Zn^{2+}, (B) Co^{2+}, (C) Ca^{2+}, (D) displacement of Co^{2+} by Zn^{2+} from 50 μM ZiCop (inset - ZiCop :
CoAc : ZnAc = 1 : 1 : 0.5, +4 charge state), (E) Pp. In case of the metals and the Pp (A through C & E), the K_ds
are determined by keeping the ZiCop concentration at 50 μM and titrating the metals and Pp in the following
concentration ranges: Zn and Co from 0 to 250 μM; Ca from 0 to 750 μM; Pp from 0 to 200 μM. For the metal
displacement experiments (D), the K_d was determined by keeping the ZiCop and CoAc concentrations at 50 μM
and titrating ZnAc from 0 to 200 μM. Hill functions are fitted to the data points and the K_d values obtained at
50% system saturation, i.e. half of the peptide population binds metal. The Kd values and number of cooperative
sites n is quoted on each panel. Data are derived from relative ion currents in ESI mass spectra (first
monoisotopic peak), summing the intensities of ion currents for all charge states of each species. Each data point
is the mean (± standard error) of the equilibrium concentrations from three mass spectra.

Visible light absorbance measurements based on the displacement of cobalt by zinc, confirm that ZiCop coordinates cobalt using a Cys_2His_2 coordination geometry, typical of classical zinc fingers [15, 47], with a K_d of around 7.5 µM. Zinc was found to displace cobalt from ZiCop, although the binding stoichiometry was found to be around 1.2:1 peptide:metal, suggesting that peptide oligomerises in the presence of the metal (see Supplementary Information). ZiCop was found to bind cobalt with lower affinity in the presence of the partner peptide, implying a lower affinity for the conformation that associates with the partner peptide. The absorbance spectrum of ZiCop in the presence of the partner peptide (Supplementary Information Figure S2) indicates that the mode of cobalt binding is unchanged.

3. *ZiCop and Partner Peptide – quantifying the strength of interaction*

For ZiCop interacting with Pp, the first assumption made above regarding the K_d measurements in the gas phase is not entirely adhered to, as the masses of both interacting partners are now very similar. However, this is well compensated by the fact that ionisation efficiencies of both (as monomers) are very similar too, so we can surmise contribution of each of them is equal. This has been confirmed by the summation of peak intensities across all charge states for each of the peptides and any homodimers from data taken at 1:1 concentrations of ZiCop and Pp. Figure 4*E* shows the binding curve of ZiCop with Pp, which is at least two orders of magnitude weaker than that found for Zn^{2+} and Co^{2+}. This is not unexpected given that coiled-coil associations are innately weaker than those of coordinated metals [48, 49]. Extrapolation of the Hill curve gives an approximate value of $K_d \approx 2 \pm 0.1$ mM. The partner peptide was also found to interact with the Zn-bound form of ZiCop, a feature that was also observed by spectroscopic experiments (Supplementary Information Figure S3).

4. ***Peptide-metal and peptide-peptide – qualitative definition of complex stability by CID***

Collision induced dissociation (CID) can probe the stability of non-covalent complexes as well as provide an indication of the specificity of non-covalent interactions [50, 51]. Here we

16

focus on two complex ions: the Zn-bound form of ZiCop interacting with Pp – Zn-ZiCop-Pp (*m/z* 1403.3) and the hetero-dimer of ZiCop and Pp – ZiCop-Pp (*m/z* 1391.0) both in their +5 charge state. Three other species were also investigated and the findings are discussed in Supplementary Information (Figure S3). As the relative dissociation energy is increased (Figure 5) complexes dissociate into their constituent parts with distinctive E_{50} values (where 50% of the precursor population has dissociated) [52, 53]. These values indicate the strength of complex association: the more energy is required to break up the interaction the more stable the complex is.

The strongest associations are observed for ZiCop interacting with Pp – in both Zn-bound and free forms (highest E_{50} values of 21 and 16 V respectively, Figure 5A and B). The stronger association between the two peptides in the presence of zinc ion is presumably a consequence of the metal-stabilised fold of ZiCop. For the Zn-ZiCop-Pp complex, the two major products are triply charged Zn-ZiCop and doubly charged Pp, for the ZiCop-Pp complex the major products are correspondingly triply charged ZiCop and doubly charged Pp albeit at lower threshold energies. Additional experiments attempting to dissociate the metal from ZiCop (data not shown) revealed that loss of Zn^{2+} is an unobservable channel, the peptide fragmented before the loss of the metal. This confirms the specific and strong interaction of zinc in ZiCop when in the Zn-ZiCop-Pp complex, and we can speculate that the interaction between Zn-ZiCop and Pp occurs *via* the α-helical part of the zinc finger fold of the ZiCop.
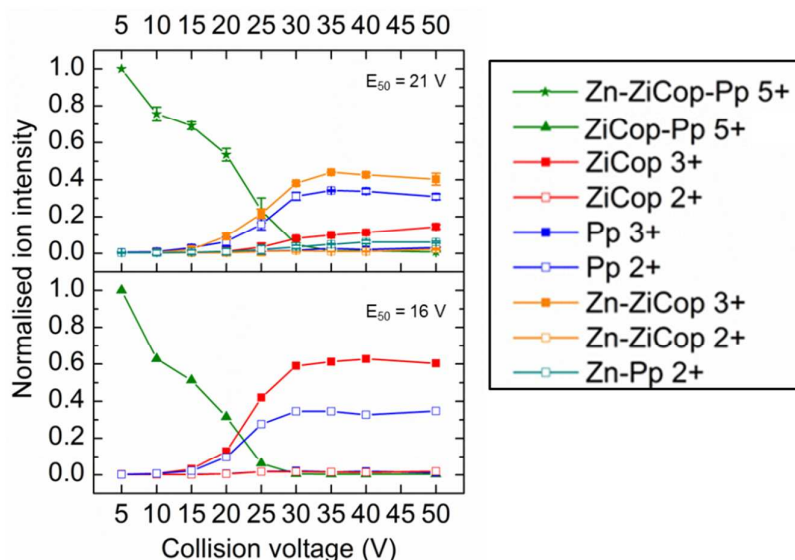
Figure 5　　　　　*Stability of non-covalent complexes as a function of dissociation energy. Fragmentation results of the following +5 charge state complexes are shown: A – Zn-ZiCop-Pp; B – ZiCop-Pp. Stability of complexes is indicated by the intensities of the precursor and product ions during CID. The green curves show dissociation of the precursor ions, all other curves are dissociation products, and the E_{50} values for the precursors are shown for each plot. Each data point is the mean (± standard error) of the equilibrium ratios from three mass spectra, the error bars are within the size of the date points.*

Comparative analysis of the dissociation curves of the metal-free hetero-dimer and two homo-dimers reveal that the strongest association is observed for the ZiCop-Pp ion (E_{50} = 16 V), followed by the Pp (E_{50} = 12 V) and ZiCop (E_{50} = 10 V) homo-dimers (cf. Figure5B and Supplementary Information Figure S3 A and B). The same order of affinity is observed in solution, a preference for hetero-dimer formation over either of the homo-dimers. Moreover, mass-spectrometry is selective enough to distinguish the interaction energies between the ZiCop and Pp self-association, with the latter possessing no sequence duality and hence a slightly stronger propensity for coiled coil formation compared to the former.

5.　***Collision cross sections and molecular dynamic simulations – elucidating conformations***

IM-MS experiments were performed on the apo and the holo forms of ZiCop and its complexes with Pp. Arrival time distributions (ATDs) at a range of drift voltages were converted to collision cross sections following Equation 1, and CCS values are presented in Table 1. For ZiCop, the cross section difference between the two charge states was around

20%, which is attributed to coulombic effects [54-56]. By contrast, the CCS for the two charge states of zinc bound ZiCop are in good agreement (Table 1*A*). This suggests the metal ion stabilised fold does not change with an additional proton. The CCS found for the hetero-dimer is significantly larger than either of the two monomer species (Table 1B), implying an elongated species rather than a globular form. This is also the case for both homo-dimers, which have very similar cross sections. The dimer of the ZiCop, however, gives a larger than expected standard error in experimental Ω values, suggesting conformational variance, possibly due to multiple inter-converting populations. This may be related to the fact that ZiCop is a *poor* coiled coil, which was the initial reason for introducing a binding partner – Pp. The +5 Zn-ZiCop-Pp dimer has larger Ω values than any of the non-metal dimers, which suggests that this is not simply a coiled-coil interaction, but is rather between the α-helical part of the zinc finger and the helix of the partner peptide. This, again, is corroborated by the CID results. The +5 dimer of Zn-ZiCop has a very similar collision cross section to the Zn-ZiCop-Pp dimer, however, there is no evidence from CID that the ZiCop forms a zinc finger fold within this arrangement, as the major fragmentation product of 2(Zn-ZiCop) is apo-ZiCop (Figure S3 C). As explained above, the loss of Zn^{2+} from Zn-ZiCop complex is an unobservable channel. If the zinc finger fold existed in the 2(Zn-ZiCop) complex, then we would expect a Zn-ZiCop to be a fragmentation product, but this is not observed as a major channel.   A plausible spatial arrangement of 2(Zn-ZiCop) in the gas phase is the one that similar to that of Zn-ZiCop-Pp, with the exception that one of the two zinc ions is not coordinated by cysteines and histidines in a zinc finger fold, but rather interacts with the charged side chains exposed by an extended form of ZiCop, acting more like Pp This hypothesis is investigated further with MD simulations (see below). It is worth noting that the 2(Zn-ZiCop) population is very small *cf* 8 % of Zn-ZiCop.

Table 1. *Experimental (IM-MS) and simulated (MD) collision cross sections of the most abundant charge states of the monomeric apo and holo-ZiCop (Zn-bound) – table A, and the dimeric species, and some of the undesirable aggregates – table B, in 'buffered' conditions. The values are quoted in $Å^2$, with standard error of three*

experimental repeats. The values for the modelled structures are shown in italics. The empty cells denote values that were not determined.

Charge state	ZiCop		Zn-ZiCop	
	IM-MS	*MD*	IM-MS	*MD*
+3	558 ± 2	*550*	648 ± 3	*645*
+4	664 ± 11	*641*	656 ± 6	

A

Charge	ZiCop-Pp		2Pp	2ZiCop	Zn-ZiCop-Pp	2(Zn-ZiCop)
	IM-MS	*MD*	IM-MS	IM-MS	IM-MS	IM-MS
+5	971 ± 24		975 ± 3	947 ± 118	1104 ± 61	1103 ± 13
+6		*1007*				

B

To support our conformational assignments, molecular dynamics (MD) simulations were performed on species shown in Table 1: apo- and holo-ZiCop and the hetero-dimer of the two – ZiCop-Pp. Figure 6 shows representative structures obtained by MD simulations. Experimental collision cross sections compare favourably with those obtained from the MD giving confidence in both datasets. Interestingly, the apo-ZiCop adopts a very similar conformation the holo-form (Figure 6A and B), with the main difference observed in the coordination sphere: the Cys and His residue side chains seem to be on the outer surface of the peptide globule in the absence of the metal ion. The α-helical portion of the peptide chain tends to be present in both apo- and holo-forms agreeing well with results obtained for an analogous peptide-based system[1]. The hetero-dimer (Figure 6C) adopts an elongated conformation consisting of the two parallel α-helices slightly twisting around each other. Although in the resulting coiled coil the termini of both chains are somewhat unstructured, the alignment of the peptides is blunt-ended as envisioned by the design.
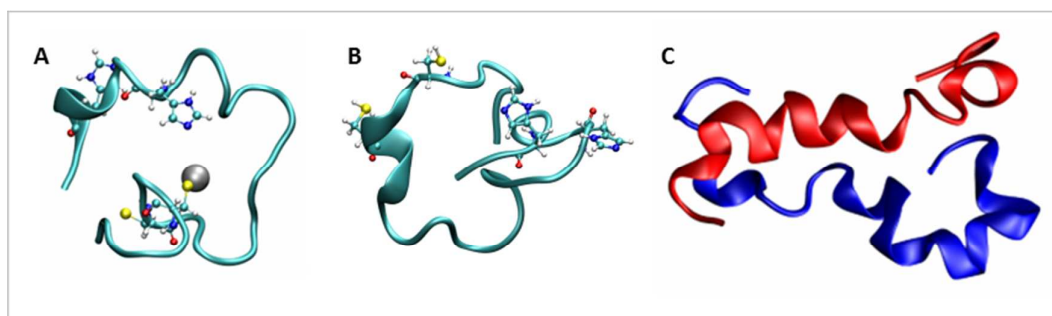

Figure6 *Representative MD structures of the +3 Zn-ZiCop (A), +3 apo-ZiCop (B) and +6 ZiCop-Pp hetero-dimer (C). Metal-coordinating residues are shown as ball-and-stick representations to highlight their role*

in the presence (A) and absence (B) of zinc ion. Hetero-dimer (C) is colour-coded according to the convention in this work to distinguish between the two interacting partners.

Conclusions

A mass spectrometry and ion-mobility mass spectrometry workflow to interrogate a protein design strategy has been presented. It has been demonstrated that MS and IM-MS can play an important role in characterising switching behaviour of a synthetic peptide-based system and informing protein design strategy in general. Specifically, attachment of a single ion effected a pronounced conformational change for ZiCop, whereby switching between two distinctly different folds was observed. The following are our primary findings:

1)   There is strong evidence that ZiCop preferentially and specifically binds Co^{2+} and, to a lesser extent Zn^{2+}, when compared to Ca^{2+}. The presence of Co^{2+}, before Zn^{2+} is added to the peptide enhances the strength of its binding by at least an order of magnitude. The shape of binding curve of Co^{2+} is sigmoidal and is similar to that of Zn^{2+}, suggesting switching behaviour of the peptide. Binding of Ca^{2+} is very weak and non-specific, with the binding curve taking a hyperbolic shape, indicating non-switching behaviour. Collision cross-sections (CCS) measurements revealed an increased conformational stability of the metal-bound ZiCop over its apo-form.

2)   IM-MS measurements and MD simulations indicate the possibility that ZiCop-Pp species adopt blunt-ended coiled coil conformations. The hetero-dimer forms preferentially over the two homo-dimers – 2ZiCop and 2Pp with a dissociation constant in the low-mM.

This work illustrates the power of a mass spectrometry approach to assist the design of functional peptides *de novo*.

Acknowledgements

References

1. Y. Berezovskaya, C. T. Armstrong, A. L. Boyle, M. Porrini, D. N. Woolfson and P. E. Barran, *Chemical Communications*, 2011, 47, 412-414.
2. C. T. Armstrong, A. L. Boyle, E. H. C. Bromley, Z. N. Mahmoud, L. Smith, A. R. Thomson and D. N. Woolfson, *Faraday Discussions*, 2009, 143, 305-317.
3. K. Yue and K. A. Dill, *Proceedings of the National Academy of Sciences of the United States of America*, 1992, 89, 4163-4167.
4. M. Dole, L. L. Mack, R. L. Hines, R. C. Mobley, L. D. Ferguson and M. B. Alice, *The Journal of Chemical Physics*, 1968, 49, 2240-2249.
5. M. Yamashita and J. B. Fenn, *The Journal of Physical Chemistry*, 2002, 88, 4451-4459.
6. J. A. Loo, *Mass Spectrometry Reviews*, 1997, 16, 1-23.
7. M. Przybylski and M. O. Glocker, *Angew. Chem., Int. Ed. Engl.*, 1996, 35, 806-826.
8. D. L. Smith and Z. Zhang, *Mass Spectrom. Rev.*, 1994, 13, 411-429.
9. D. E. Clemmer and M. F. Jarrold, *Journal of Mass Spectrometry*, 1997, 32, 577-592.
10. B. T. Ruotolo, K. Giles, I. Campuzano, A. M. Sandercock, R. H. Bateman and C. V. Robinson, *Science*, 2005, 310, 1658-1661.
11. J. A. Loo, B. Berhane, C. S. Kaddis, K. M. Wooding, Y. Xie, S. L. Kaufman and I. V. Chernushevich, *Journal of the American Society for Mass Spectrometry*, 2005, 16, 998-1008.
12. D. R. Engelke, S.-Y. Ng, B. S. Shastry and R. G. Roeder, *Cell*, 1980, 19, 717-728.
13. W. Li, J. Zhang, J. Wang and W. Wang, *Journal of the American Chemical Society*, 2008, 130, 892-900.
14. S. Iuchi and N. Kuldell, *Zinc Finger Proteins: From Atomic Contact to Cellular Function*, Plenum Publishers, 2005.
15. S. S. Krishna, I. Majumdar and N. V. Grishin, *Nucl. Acids Res.*, 2003, 31, 532-550.
16. A. Klug, *Annual Review of Biochemistry*, 2010, 79, 213-231.
17. A. H. Fox, C. Liew, M. Holmes, K. Kowalski, J. Mackay and M. Crossley, *EMBO J*, 1999, 18, 2812-2822.
18. F. Crick, *Acta Crystallographica*, 1953, 6, 689-697.
19. G. Grigoryan and A. E. Keating, *Current Opinion in Structural Biology*, 2008, 18, 477-483.
20. D. N. Woolfson and T. Alber, *Protein Science*, 1995, 4, 1596-1607.
21. D. Krylov, J. Barchi and C. Vinson, *Journal of Molecular Biology*, 1998, 279, 959-972.
22. J. M. Mason and K. M. Arndt, *ChemBioChem*, 2004, 5, 170-176.
23. R. Beveridge, S. Covill, K. J. Pacholarz, J. M. Kalapothakis, C. E. MacPhee and P. E. Barran, *Anal Chem*, 2014, DOI: 10.1021/ac5027435.
24. B. Domon and R. Aebersold, *Science*, 2006, 312, 212-217.
25. K. J. Pacholarz, R. A. Garlish, R. J. Taylor and P. E. Barran, *Chem Soc Rev*, 2012, 41, 4335-4355.
26. E. J. Want, B. F. Cravatt and G. Siuzdak, *Chembiochem : a European journal of chemical biology*, 2005, 6, 1941-1951.
27. L. Konermann, J. Pan and D. J. Wilson, *BioTechniques*, 2005, 40, 135,137,139,141.
28. C. Afonso, Y. Hathout and C. Fenselau, *J. Mass Spectrom.*, 2002, 37, 755-759.

29. D. E. Clemmer, R. R. Hudgins and M. F. Jarrold, *Journal of the American Chemical Society*, 1995, 117, 10141-10142.

30. J. L. P. Benesch, B. T. Ruotolo, D. A. Simmons and C. V. Robinson, *Chemical Reviews*, 2007, 107, 3544-3567.

31. M. Sharon and C. V. Robinson, *Annual Review of Biochemistry*, 2007, 76, 167-193.

32. S. J. Valentine, A. E. Counterman and D. E. Clemmer, *Journal of the American Society for Mass Spectrometry*, 1999, 10, 1188-1211.

33. M. De Cecco, E. S. Seo, D. J. Clarke, B. J. McCullough, K. Taylor, D. Macmillan, J. R. Dorin, D. J. Campopiano and P. E. Barran, *The Journal of Physical Chemistry B*, 2010, 114, 2312-2318.

34. T. Wyttenbach and M. T. Bowers, *Annual Review of Physical Chemistry*, 2007, 58, 511-533.

35. M. F. Mesleh, J. M. Hunter, A. A. Shvartsburg, G. C. Schatz and M. F. Jarrold, *The Journal of Physical Chemistry*, 1996, 100, 16082-16086.

36. A. A. Shvartsburg and M. F. Jarrold, *Chemical Physics Letters*, 1996, 261, 86-91.

37. T. Wyttenbach, G. vonHelden, J. J. Batka, D. Carlat and M. T. Bowers, *Journal of the American Society for Mass Spectrometry*, 1997, 8, 275-282.

38. C. T. Armstrong, Ph.D., University of Bristol, 2010.

39. K. A. Sannes-Lowery, R. H. Griffey and S. A. Hofstadler, *Analytical Biochemistry*, 2000, 280, 264-271.

40. B. J. McCullough, J. Kalapothakis, H. Eastwood, P. Kemper, D. MacMillan, K. Taylor, J. Dorin and P. E. Barran, *Analytical Chemistry*, 2008, 80, 6336-6344.

41. J. T. Moseley, I. R. Gatland, D. W. Martin and E. W. McDaniel, *Physical Review*, 1969, 178, 234.

42. J. Myers, G. Grothaus, S. Narayanan and A. Onufriev, *Proteins: Structure, Function, and Bioinformatics*, 2006, 63, 928-938.

43. D. V. Sakharov and C. Lim, *Journal of the American Chemical Society*, 2005, 127, 4921-4929.

44. V. Gabelica, N. Galic, F. Rosu, C. Houssier and E. De Pauw, *J. Mass Spectrom.*, 2003, 38, 491-501.

45. E. Boeri Erba, K. Barylyuk, Y. Yang and R. Zenobi, *Analytical Chemistry*, 2011, 83, 9251-9259.

46. S. L. Shirran and P. E. Barran, *Journal of the American Society for Mass Spectrometry*, 2009, 20, 1159-1171.

47. J. H. Laity, B. M. Lee and P. E. Wright, *Current Opinion in Structural Biology*, 2001, 11, 39-46.

48. J. R. Litowski and R. S. Hodges, *Journal of Biological Chemistry*, 2002, 277, 37272-37279.

49. A. R. Reddi, T. R. Guzman, R. M. Breece, D. L. Tierney and B. R. Gibney, *Journal of the American Chemical Society*, 2007, 129, 12815-12827.

50. R. D. Smith, J. E. Bruce, Q. Wu and Q. P. Lei, *Chem. Soc. Rev.*, 1997, 26, 191-202.

51. A. J. R. Heck and T. J. D. Jørgensen, *International Journal of Mass Spectrometry*, 2004, 236, 11-23.

52. J. L. P. Benesch, J. A. Aquilina, B. T. Ruotolo, F. Sobott and C. V. Robinson, *Chemistry & Biology*, 2006, 13, 597-605.

53. C. V. Robinson, E. W. Chung, B. B. Kragelund, J. Knudsen, R. T. Aplin, F. M. Poulsen and C. M. Dobson, *Journal of the American Chemical Society*, 1996, 118, 8646-8653.

54. K. B. Shelimov, D. E. Clemmer, R. R. Hudgins and M. F. Jarrold, *Journal of the American Chemical Society*, 1997, 119, 2240-2248.

55. S. J. Valentine, J. G. Anderson, A. D. Ellington and D. E. Clemmer, *The Journal of Physical Chemistry B*, 1997, 101, 3891-3900.

56. T. Covey and D. J. Douglas, *J. Am. Soc. Mass Spectrom.*, 1993, 4, 616-623.
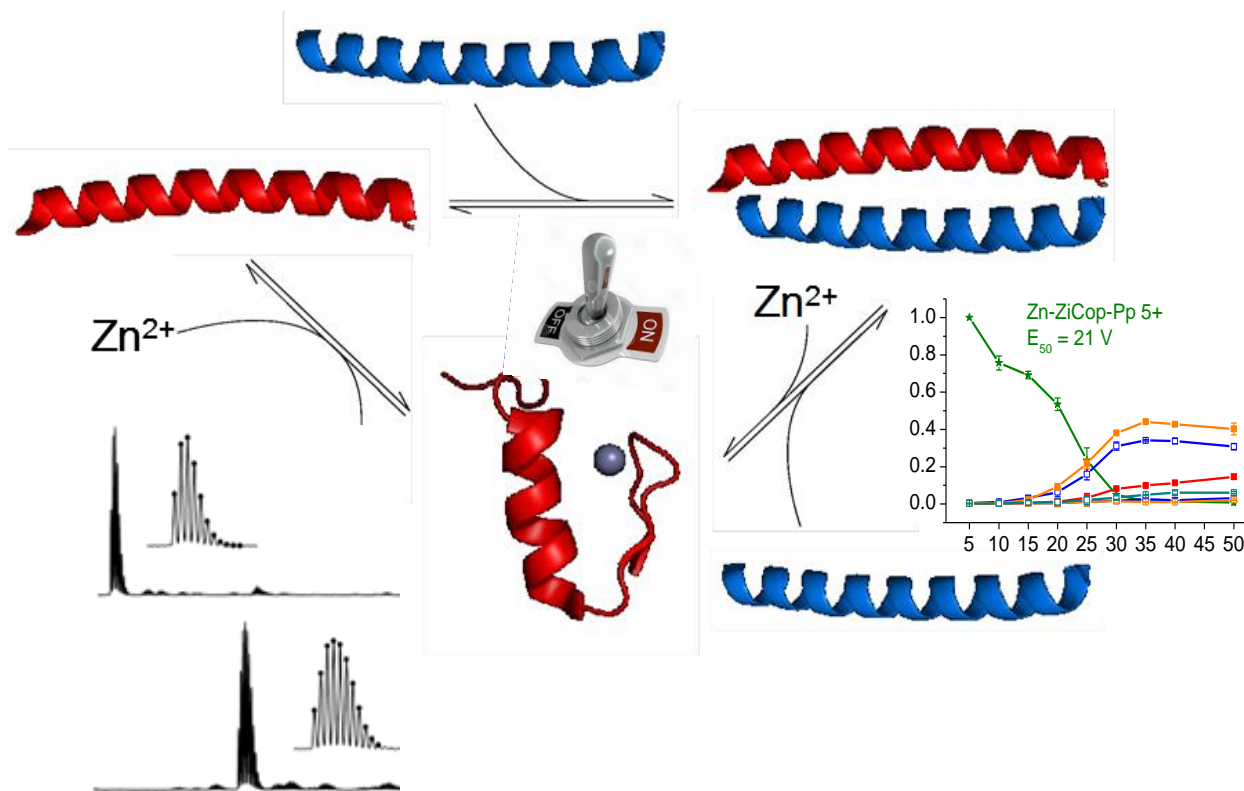
A combination of affinity mass spectrometry, collisional activation and ion mobility analysis coupled with molecular dynamics measurements, are used to probe a zinc finger –coiled coil switching peptide system.